Efficient numerical method for solving the direct Zakharov–Shabat scattering problem

Leonid L. Frumin,[1,2] Oleg V. Belai,[1] Eugeny V. Podivilov,[1,2] and David A. Shapiro[1,2,*]

[1]*Institute of Automation and Electrometry, Siberian Branch, Russian Academy of Sciences, Novosibirsk 630090, Russia*
[2]*Novosibirsk State University, Novosibirsk 630090, Russia*
**Corresponding author: shapiro@iae.nsk.su*

Received October 28, 2014; revised December 15, 2014; accepted December 15, 2014;
posted December 15, 2014 (Doc. ID 225812); published January 15, 2015

A new method to solve the direct Zakharov–Shabat scattering problem is proposed based on the solution for coupled Gel'fand–Levitan–Marchenko integral equations. Speedup of computations is achieved by using the Töplitz symmetry of the matrix and an "inner bordering" procedure. The new algorithm was tested on the exactly solvable potential. It is shown that the suggested algorithm significantly surpasses the traditional transfer matrix method in efficiency.

OCIS codes: (000.3860) Mathematical methods in physics; (290.3200) Inverse scattering; (190.4370) Nonlinear optics, fibers; (060.3735) Fiber Bragg gratings.
http://dx.doi.org/10.1364/JOSAB.32.000290

1. INTRODUCTION

The modeling of modern optical communication links, especially with back-propagation technology, requires fast and accurate methods for solving the nonlinear Shrödinger equation (NLSE) [1]. Experience gathered over a number of years points out that the finite difference and pseudo-spectral methods [2,3] are the best. One of the most efficient methods among them is the split-step Fourier method (SSFM) that determines the solution after $O(NM \log N)$ operations. Here, M, N are the dimensions of the problem in space and time, respectively. In communications, both dimensions can obtain values as high as $2^{15}/2^{18}$ and more. The symmetric splitting scheme makes it possible to achieve second-order accuracy in both the variables. Therefore, this approach is widely used in modeling of signal propagation. The advantage of the SSFM is its universality, i.e., the method is suitable both for forward and backward propagation in communication lines with amplification and damping. At the same time, the high computational difficulty excludes its real-time exploitation in practice. Note that a significant speedup of pseudo-spectral methods is provided by the parallel algorithms [4,5], but this approach is also far from being applied regularly in communications.

An alternative is the inverse scattering transform (IST) or nonlinear Fourier transform method [6–8]. The solution of the NLSE with these methods is reduced to three steps: (i) solving the direct scattering problem attributed to Zakharov–Shabat equations (ZSE) for the potential distribution resembling the initial condition, (ii) propagation of the scattering data to the other end, and (iii) solving the inverse scattering problem for propagated scattering data. The inverse scattering problem is solved by the layer-peeling method [9–12] that comes from geophysics and electronics. The method requires $O(M^2)$ operations. The layer-peeling method, however, has the first-order accuracy $O(M^{-1})$ and its application gives no speed gain compared to the SSFM at the same target accuracy. The same is valid for most other methods [13–17]. Different inverse scattering algorithms were compared in an earlier paper [18] in terms of their robustness, speed, and implementation difficulties.

Rather recently, the authors suggested a so-called Töplitz inner bordering (TIB) method [19] for the numerical solution of the Gel'fand–Levitan–Marchenko (GLM) coupled integral equations [20]. It was successfully applied to the problem of fiber Bragg grating (FBG) synthesis. The method is as fast as the layer peeling and requires $O(M^2)$ operations, but it provides second-order accuracy $O(M^{-2})$. The method is based on the Töplitz symmetry of the discretized equations and includes the bordering procedure analogous to the Levinson–Durbin or Trench recursion [21–23] (see also [24,25]). In contrast to previous algorithms that aim to invert a general Töplitz matrix by applying the original bordering procedure, we account for a special block structure of our coefficient matrix by introducing "inner bordering." That method was tested numerically and appeared to be accurate and stable with respect to noise even for high-reflectance gratings compared to the layer peeling [26]. The method also has been applied successfully to the inverse synthesis for high spectral efficiency transmission in optical fibers [27]. However, the method solves only the inverse problem while the direct problem is solved by the standard T-matrix method (see [28,29]).

The aim of the present paper is to introduce a new method for the direct problem. It is based on GLM integral equations and uses the Töplitz symmetry of the matrix. The new method is shown to be more efficient than the T-matrix method. Note that the idea to solve the direct scattering problem with the help of GLM equations is mentioned in the book by Lamb [30].

In Section 2, we review the basic points of the inverse scattering transform for ZSE (in FBG theory, the coupled mode equations). Section 3 describes the inner bordering method for the GLM set. The new method for ZSE is introduced in Section 4. In Section 5, an exact solution of ZSE is used to test the method efficiency. We compare the new method with

the well-known T-matrix method and reveal its advantages. Finally, Section 6 summarizes our conclusions. The details involved in proving the second-order approximation are given in Appendix A.

2. SCATTERING PROBLEM

To be specific, we consider the left scattering problem for the one-dimensional potential within the segment $x \in [0, L]$. The incident wave with amplitude $a_1(x)$ gives birth to the reflected wave $a_2(x)$. The amplitudes satisfy the ZSE:

$$\frac{da_1}{dx} + i\omega a_1 = q(x)a_2, \qquad \frac{da_2}{dx} - i\omega a_2 = \pm q^*(x)a_1, \tag{1}$$

where ω is the spatial frequency, x is the coordinate, $q(x)$ is the coupling coefficient (complex potential), and the asterisk denotes the complex conjugation. The boundary conditions for the left scattering problem are $a_1(0) = 1, a_2(L) = 0$, then the reflection and transmission coefficients are $r = a_2(0)$, $d = a_1(L)$. The direct scattering problem consists of determining the complex reflection coefficient $r(\omega)$ from the given potential $q(x)$.

Signs "+" and "−" in communications correspond to fibers with normal and anomalous dispersions, respectively. If the sign is "−," then the discrete spectrum may exist and be responsible for the solitons of the NLSE. In the problem of laser beam self focusing, the NLSE with different signs is called "defocusing" or "focusing" nonlinearity. When the discrete spectrum exists, the positions of poles of the coefficient and residues in these poles are added to the required scattering data.

In numerical calculations, the segment is usually divided by M uniform layers with dimension $h = L/M$. The column vector of amplitudes $\psi(x) = (a_1(x), a_2(x))^T$ (here, T denotes the transpose) at the right and left ends of the layer are bound by linear relations:

$$\psi(x + h) = \mathbf{T}\psi(x), \qquad \mathbf{T} = \begin{pmatrix} a & b \\ \pm b^* & a^* \end{pmatrix}. \tag{2}$$

Matrix $\mathbf{T}$ is known as the T-matrix or transfer matrix. For the upper sign in Eq. (1), its elements are

$$a = \cosh \mu h - i\frac{\omega}{\mu} \sinh \mu h, \qquad b = \frac{q}{\mu} \sinh \mu h, \tag{3}$$

where $\mu = \sqrt{|q|^2 - \omega^2}$, and the matrix is pseudo-unitary: $|a|^2 - |b|^2 = 1$. For the lower sign, they are

$$a = \cos \mu h - i\frac{\omega}{\mu} \sin \mu h, \qquad b = \frac{q}{\mu} \sin \mu h, \tag{4}$$

where $\mu = \sqrt{|q|^2 + \omega^2}$, and $\mathbf{T}$ is unitary: $|a|^2 + |b|^2 = 1$. In both of the cases, the determinant of the T-matrix is equal to unity: $\det \mathbf{T} = |a|^2 \mp |b|^2 = 1$. The sequential multiplication of T-matrices of all the layers gives the numerical solution of the scattering problem [31]. If one assigns the transfer matrix to the center of each layer, then the calculations have the second-order accuracy $O(h^2) \equiv O(M^{-2})$. Since we should multiply T-matrices over the whole spectral interval involving M harmonics, the required number of operations is $O(M^2)$.

3. INNER BORDERING

The inverse scattering problem is to find the potential $q(x)$ from the known scattering data. In our case, the scattering data involve the complex reflection coefficient $r(\omega)$ as a function of the frequency. For the known limitation of the potential behavior at infinity $\int |q(x)|(1 + |x|)\mathrm{d}x < \infty$, the inverse scattering problem reduces to the pair of coupled GLM equations [20,30] (see also [16]):

$$\begin{aligned} &A_1^*(x, y) + \int_{-y}^{x} A_2(x, z)R(y + z)\mathrm{d}z = 0, \\ &\pm A_2^*(x, y) + \int_{-y}^{x} A_1(x, z)R(y + z)\mathrm{d}z + R(x + y) = 0, \\ &\qquad -x \le y < x, \qquad 0 \le x \le L. \end{aligned} \tag{5}$$

One looks for two unknown complex functions $A_{1,2}$ from Eq. (9), while the (modified) impulse response $R(x)$ is known:

$$R(x) = \frac{1}{2\pi}\int_{-\infty}^{\infty} r(\omega)e^{-i\omega x}\mathrm{d}\omega, \tag{6}$$

where $r(\omega)$ is the complex reflection coefficient. For the lower sign in Eq. (1), the sum of residues should be added to Eq. (6) when there is a discrete spectrum [30]. The following synthesis relation gives the potential in terms of function A_2:

$$q(x) = \pm 2A_2^*(x, x - 0). \tag{7}$$

After the complex conjugation of the first Eq. (5) and introducing the new unknown functions as

$$u(x, s) = A_1(x, x - s), \tag{8}$$

$$v(x, \tau) = \pm A_2^*(x, \tau - x), \tag{9}$$

we get the modified GLM set:

$$\begin{aligned} &u(x, s) \pm \int_{s}^{2x} R^*(\tau - s)v(x, \tau)\mathrm{d}\tau = 0, \\ &v(x, \tau) + \int_{0}^{\tau} R(\tau - s)u(x, s)\mathrm{d}s + R(\tau) = 0, \\ &\qquad 0 \le s, \tau < 2x, \qquad 0 \le x \le L, \end{aligned} \tag{10}$$

and the synthesis relation $q(x) = 2v(x, 2x - 0)$.

The numerical method suggested in [19] is based on Eq. (10), which is reduced to a sequence of sets of linear algebraic equations with Töplitz and Hermitian coefficient matrices possessing a special block structure. The dimensions of the sequence members grow with parameter x. The Hermitian form of the matrix was exploited in the algorithm with $O(M^3)$ complexity and $O(M^{-1})$ accuracy [32]. The Töplitz symmetry was recognized in an earlier paper [19] where the GLM equations were reduced to the set of Eq. (10) with the difference kernel.

The bordering procedure elaborated for a Töplitz matrix decreases the number of operations by an order of magnitude compared to the general Gauss method for every equation set in the sequence. The intermediate results obtained for any sequence member are reused for its follower. Additional one-order economy is achieved because of the fact that only one element of the solution vector is needed. As a result, the

complexity has decreased up to $O(M^2)$ required operations. The accuracy has been improved to $O(M^{-2})$.

In Ref. [19], the second-order accuracy $O(M^{-2})$ was demonstrated numerically. However, there was no derivation of the working formulas. Instead of the derivation, a receipt was given to take the right part in the middle points instead of the grid nodes. This implies a shift by half a step in the coordinate for the unknown functions. This receipt is incomplete; namely, along with the right part modification, one must extrapolate the solution to the interval ends. The omitted derivation, proof, and definitions of the grid functions are carried out in Appendix A of the present paper.

The numerical efficiency of the algorithm is defined in the main by the symmetry properties of the inverse matrix. When the direct matrix $\mathbf{G}$ becomes non-Hermitian, the inverse matrix $\mathbf{G}^{-1}$ is neither Hermitian nor anti-Hermitian. At first glance, it should diminish the efficiency of the algorithm. However, both matrices $\mathbf{G}$ and $\mathbf{G}^{-1}$ have a block structure (see Appendix A), particularly,

$$\mathbf{G} = \begin{pmatrix} \mathbf{E} & \pm\mathbf{R}^\dagger \\ \mathbf{R} & \mathbf{E} \end{pmatrix}. \tag{11}$$

Here † means the Hermitian conjugation. Then, the efficiency is determined by the symmetry of the blocks. The left inverse matrix [33] for Eq. (11) is

$$\mathbf{G}^{-1} = \begin{pmatrix} (\mathbf{E}\mp\mathbf{R}^\dagger\mathbf{R})^{-1} & \mp(\mathbf{E}\mp\mathbf{R}^\dagger\mathbf{R})^{-1}\mathbf{R}^\dagger \\ -(\mathbf{E}\mp\mathbf{R}\mathbf{R}^\dagger)^{-1}\mathbf{R} & (\mathbf{E}\mp\mathbf{R}\mathbf{R}^\dagger)^{-1} \end{pmatrix}. \tag{12}$$

From Eq. (12), it is apparent that in the normal dispersion case (the upper sign in formulas) all the blocks are Hermitian. In the case of anomalous dispersion (the lower signs), the diagonal blocks are Hermitian, while the off-diagonal blocks are anti-Hermitian. Thus, the degree of symmetry remains high for anomalous dispersion.

The TIB algorithms for normal and anomalous dispersion differ by signs only. The basics for the algorithm are relations between the left and right columns of the inverse matrix f_1, f_m and between the top and bottom matrix rows g_1, g_m. Töplitz symmetry of matrix $\mathbf{G}$ results in the persymmetric inverse matrix $\mathbf{G}^{-1}$. Let us denote y, z half-columns of the left column of the inverse matrix:

$$f_1 = \begin{pmatrix} y \\ z \end{pmatrix}. \tag{13}$$

For the Hermitian case, the top row g_1 is the Hermitian conjugate to the left column f_1. In the general case, the top row is

$$g_1 = \begin{pmatrix} y^{T*} & \pm z^{T*} \end{pmatrix}. \tag{14}$$

The inverse matrix is then persymmetric and its bottom row has the form

$$g_m = \begin{pmatrix} \tilde{z}^T & \tilde{y}^T \end{pmatrix}, \tag{15}$$

where the tilde stands for the inverse numeration of the indices. The right column is analogously given by

$$f_m = \begin{pmatrix} \pm\tilde{z}^* \\ \tilde{y}^* \end{pmatrix}. \tag{16}$$

Equations (13)–(16) help to build up the high efficiency bordering algorithm. The algorithm uses Hermitian or anti-Hermitian symmetry of blocks of inverse matrix $\mathbf{G}^{-1}$ and the Töplitz symmetry of matrix $\mathbf{G}$.

The second-order algorithm for the inverse scattering problem consists of the following steps.

(1) Let $m = 1$, calculate $q_0 = -2R_0$, and give auxiliary vectors their initial values:

$$y_0^{(1)} = \frac{1}{1\mp h^2|R_0|^2/4}, \qquad z_0^{(1)} = -\frac{y_0^{(1)} h R_0}{2}. \tag{17}$$

(2) Find the main parameter of the algorithm:

$$\beta_m = h\sum_{j=0}^{m-1} R_{m-j} y_j^{(m)}. \tag{18}$$

(3) Find the potential; this is the output at every step:

$$q_m = -2\beta_m/h. \tag{19}$$

(4) Calculate coefficients:

$$c_m = \frac{1}{1\mp|\beta_m|^2}, \qquad d_m = -\beta_m c_m. \tag{20}$$

(5) Determine the auxiliary vectors:

$$\mathbf{y}^{(m+1)} = c_m\begin{pmatrix} \mathbf{y}^{(m)} \\ 0 \end{pmatrix} + d_m\begin{pmatrix} 0 \\ \pm\tilde{\mathbf{z}}^{*(m)} \end{pmatrix},$$
$$\mathbf{z}^{(m+1)} = c_m\begin{pmatrix} \mathbf{z}^{(m)} \\ 0 \end{pmatrix} + d_m\begin{pmatrix} 0 \\ \tilde{\mathbf{y}}^{*(m)} \end{pmatrix}. \tag{21}$$

(6) With increment m, go to step 2.

4. ALGORITHM FOR THE DIRECT PROBLEM

The algorithm for the inverse scattering problem described in Section 3 can be inverted to solve the direct scattering problem. The computational process can be written with the following scheme.

(1) Let $m = 1$, calculate $R_0 = -q_0/2$, and give auxiliary vectors their initial values with Eq. (17).

(2) Find the main parameter of the algorithm:

$$\beta_m = -hq_m/2. \tag{22}$$

(3) Find the (modified) impulse response; this is the output at every step:

$$R_m = \left(\beta_m - h\sum_{j=0}^{m-1} R_{m-j} y_j^{(m)}\right)/y_0^{(m)}. \tag{23}$$

(4) Calculate the coefficients c_m, d_m with Eq. (20).

(5) Determine the auxiliary vectors $\mathbf{y}^{(m+1)}, \mathbf{z}^{(m+1)}$ by Eq. (21).

(6) With increment m, go to step 2.

The cycle stops at $m = M$. The impulse response is then Fourier-transformed to get the complex reflection coefficient if the discrete spectrum is absent.

5. COMPARISON WITH THE T-MATRIX METHOD

To test the new algorithm, we solve the direct scattering problem by the well-known T-matrix method with an exactly solvable case [34] for defocusing ZSE:

$$q(x) = \frac{Q}{\Lambda}\left(\operatorname{sech}\frac{x}{\Lambda}\right)^{1-2iF}, \tag{24}$$

where Q, F are the amplitude and phase modulation parameters, respectively, and Λ is the characteristic length. The complex reflection coefficient is given by

$$r(\omega) = -2^{-2iF}Q\frac{\Gamma(d)}{\Gamma(d^*)}\frac{\Gamma(f_-)}{\Gamma(g_-)}\frac{\Gamma(f_+)}{\Gamma(g_+)}, \tag{25}$$

where arguments of the Euler gamma-function [35] are given by relations:

$$\begin{aligned} d &= \frac{1}{2} + i[\omega\Lambda - F], \\ f_\pm &= \frac{1}{2} - i\left[\omega\Lambda \pm \sqrt{F^2+Q^2}\right], \\ g_\pm &= 1 - i\left[F \pm \sqrt{F^2+Q^2}\right]. \end{aligned} \tag{26}$$

The reflection spectrum is expressed in terms of elementary functions:

$$|r(\omega)|^2 = \frac{\cosh 2\pi\sqrt{Q^2+F^2} - \cosh 2\pi F}{\cosh 2\pi\sqrt{Q^2+F^2} + \cosh 2\pi\omega\Lambda}. \tag{27}$$

The example of potential is shown in Fig. 1. Figure 2 shows the corresponding reflection coefficient as a function of wavenumber ω via Eq. (25). The impulse response, which is defined as the Fourier transform of the reflection coefficient, is presented in Fig. 3.

Figure 4 compares the approximation order of the two methods. The standard deviation for the impulse response from the discrete Fourier transform of the analytical solution is plotted:

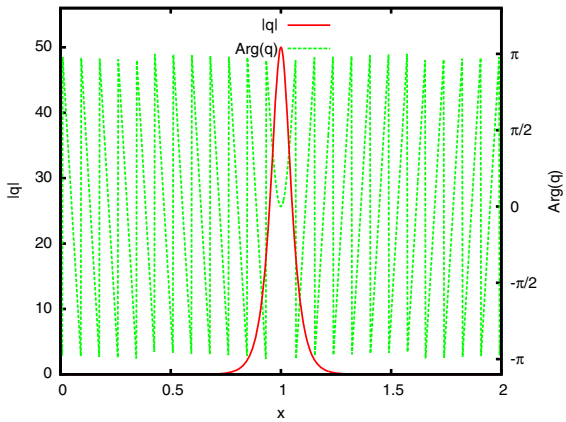

Fig. 1. Absolute value $|q|$ (solid line) and phase Arg(q) (dashed) of potential Eq. (24) values as functions of coordinate x at $F = 1.5$, $Q = 2$, $L = 2$, $\Lambda = 1/25$.

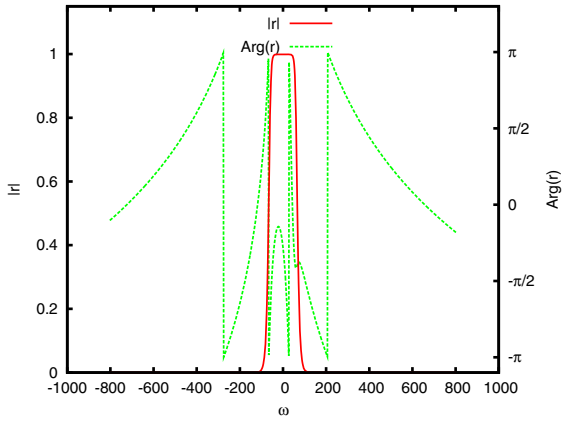

Fig. 2. Reflection spectrum $r(\omega)$ from Eq. (25): absolute value $|r|$ (solid line) and phase Arg(r) (dashed).

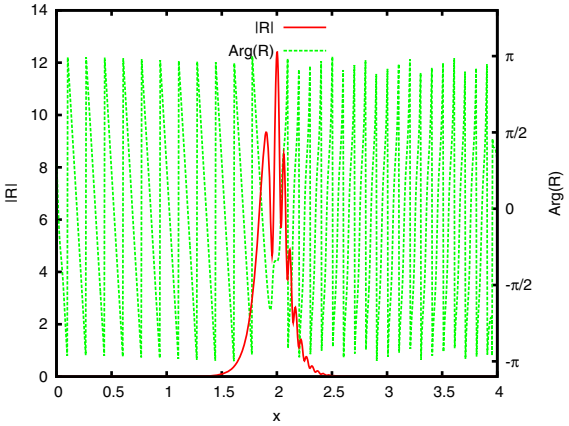

Fig. 3. Absolute value $|R|$ (solid line) and phase Arg(R) (dashed) of the impulse response as functions of coordinate x at $F = 1.5$, $Q = 2$, $L = 2$, $\Lambda = 1/25$.

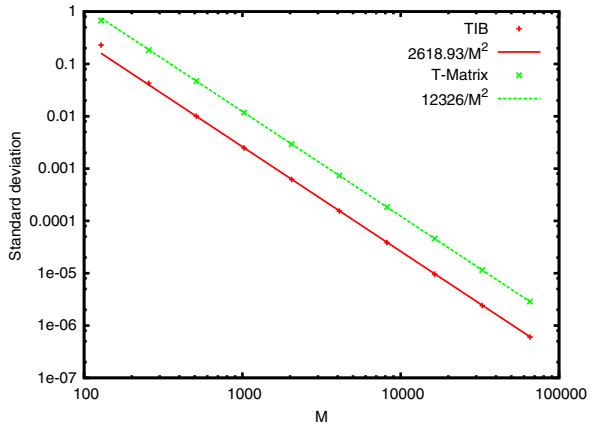

Fig. 4. Standard deviation for the new method (+) and T-matrix method (x) along with least-squares fitting to a quadratic function (solid and dashed lines, respectively).

$$\sigma = \sqrt{\frac{1}{M}\sum_{j=1}^{M}|R_j - \mathcal{F}[r(\omega)]_j|^2}, \tag{28}$$

where R_j is the impulse response at point j, $r(\omega)$ is the complex reflection coefficient (analytical solution), $\mathcal{F}[\ldots]_j$ is the

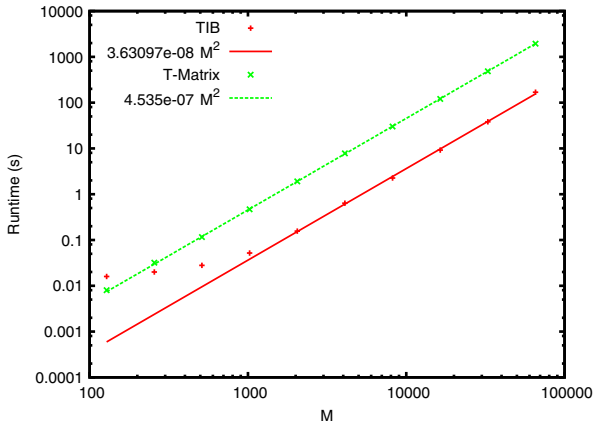

Fig. 5. Runtime (in seconds) for the new method (+) and T-matrix method (x) along with least-squares fitting to a quadratic function (solid and dashed lines, respectively).

Fourier transform obtained numerically at point j. For comparison, the fitted inverse quadratic dependence M^{-2} for each set is shown by a straight line in logarithmic coordinates.

Along with the data for the TIB (pluses) and T-matrix (crosses) methods, the least-squares fitting to quadratic functions are presented. The fitted curves make it clear that both methods provide the second-order approximation (the error falls as M^{-2} with growing number of points M). Besides that, one can see that the new method is about 4.7 times more accurate than the T-matrix method for $Q = 2$. Comparison with higher reflection potential at $Q = 4$ demonstrates that the error of both methods increases differently (by about 3 times for the T-matrix method and about 20 times for the new one) with the new method going less accurate. For high-reflection potential, the error increases while the runtime is independent of potential parameters. For very strong gratings at $1 - |r|^2 \ll 1$, all the methods lose their accuracy, since an eigenvalue of the GLM equations tends to zero and the problem becomes ill-conditioned. Comparison of the runtimes in Fig. 5 shows that both methods require M^2 operations but the new method is about 12.5 times faster.

Recently, a very fast method of forward scattering transform has been proposed [36] that achieves $O(M \log^2 M)$ runtime, where M is the number of sample points. The application of this method could decrease the runtime throughout the solution of the direct problem, but it has no influence on the solution of the inverse problem.

6. CONCLUSIONS

A new numerical algorithm is proposed to solve the scattering problem for focusing and defocusing Zakharov–Shabat equations. It is closely related to the TIB method for the coupled GLM equations and is based on Töplitz symmetry and an inner bordering procedure. The method is fast ($\sim M^2$ operations) and accurate ($\sim M^{-2}$ approximation). The calculation speed exceeds that of the known T-matrix method by about 10 times. This algorithm can be applied as a part of the inverse scattering method that is a promising candidate tool for numerical simulations of modern optical communication lines.

APPENDIX A: GROUNDING OF THE NUMERICAL ALGORITHM

Substitute continuous independent variables s, τ, x in Eq. (10) with discrete grids dividing their domains by M segments:

$$\begin{aligned} &s_k = hk, \qquad \tau_n = hn, \qquad n,k = 0,\dots,m,\\ &x_m = hm/2, \qquad m = 1,\dots,M,\\ &h = 2L/M. \end{aligned} \tag{A1}$$

Changing the integrals in Eq. (10) by finite sums according to the trapezium rule, we get the following algebraic equations:

$$\begin{aligned} &u_0^{(1)} = 0, \qquad v_0^{(1)} = -R_0,\\ &u_k^{(m)} + \frac{h}{2}R_0^* v_k^{(m)} \pm h\sum_{n=k+1}^{m-1} R_{n-k}^* v_n^{(m)} \pm \frac{h}{2}R_{m-k}^* v_m^{(m)} = 0,\\ &v_n^{(m)} + \frac{h}{2}R_n u_0^{(m)} + h\sum_{k=1}^{n-1} R_{n-k} u_k^{(m)} + \frac{h}{2}R_0 u_n^{(m)} = -R_n,\\ &n,k = 0,\dots,m, \qquad m = 1,\dots,M. \end{aligned} \tag{A2}$$

The coefficient matrix of this equation set is apparently neither Töplitz nor Hermitian, which makes it impossible to apply known efficient methods for matrix inversion. However, omitting the equations at $n,k = 0$ and taking some terms to the right part, we can make the matrix Töplitz and Hermitian, albeit at the cost of unknowns residing in the right part:

$$\begin{aligned} &u_k^{(m)} \pm \frac{h}{2}R_0^* v_k^{(m)} \pm h\sum_{n=k+1}^{m} R_{n-k}^* v_n^{(m)} = \pm\frac{h}{2}R_{m-k}^* v_m^{(m)},\\ &v_n^{(m)} + h\sum_{k=1}^{n-1} R_{n-k} u_k^{(m)} + \frac{h}{2}R_0 u_n^{(m)} = -R_n - \frac{h}{2}R_n u_0^{(m)},\\ &\quad n,k = 1,\dots,m, \qquad m = 1,\dots,M. \end{aligned} \tag{A3}$$

Thorough inspection of this equation set shows the following:

(1) It has a symmetric block structure, but with an exception—the indices of R_{m-k}^* and R_n run from m to 0 and from 1 to $m-1$, respectively.

(2) It is not closed since the right part contains $u_0^{(m)}$, the equation of which was previously omitted.

To treat these two issues, we can substitute within the second-order accuracy:

$$\begin{aligned} &\frac{h}{2}R_{m-k}^* v_m^{(m)} = \frac{h}{2}R_{m-k+1}^* v_m^{(m)} + O(h^2),\\ &\frac{h}{2}R_n u_0^{(m)} = \frac{h}{2}R_n u_1^{(m)} + O(h^2). \end{aligned} \tag{A4}$$

We can now rewrite the resultant equations in matrix form [omitting upper indices (m) in vectors and matrices]:

$$\mathbf{G}\begin{pmatrix}\mathbf{u}\\ \mathbf{v}\end{pmatrix} = \begin{pmatrix}\mathbf{a}\\ \mathbf{b}\end{pmatrix}, \tag{A5}$$

$$\mathbf{G}=\begin{pmatrix}\mathbf{E} & \pm\mathbf{R}^{\dagger}\\ \mathbf{R} & \mathbf{E}\end{pmatrix},\qquad \mathbf{R}=h\begin{pmatrix}\frac{1}{2}R_0 & 0 & \cdots & 0\\ R_1 & \frac{1}{2}R_0 & \cdots & 0\\ \vdots & \vdots & \ddots & \vdots\\ R_{m-1} & R_{m-2} & \cdots & \frac{1}{2}R_0\end{pmatrix},$$

$$\mathbf{a}=\pm\frac{h}{2}v_m^{(m)}\tilde{\boldsymbol{\rho}}^{*},\qquad \mathbf{b}=-\left(1+\frac{h}{2}u_1^{(m)}\right)\boldsymbol{\rho},$$

$$\boldsymbol{\rho}=\begin{pmatrix}R_1\\ \vdots\\ R_m\end{pmatrix},\qquad \mathbf{u}=\begin{pmatrix}u_1^{(m)}\\ \vdots\\ u_m^{(m)}\end{pmatrix},\qquad \mathbf{v}=\begin{pmatrix}v_1^{(m)}\\ \vdots\\ v_m^{(m)}\end{pmatrix}. \tag{A6}$$

Here, $\mathbf{E}$ is the identity matrix.

Multiplication of the first row g_1 from Eq. (15) and the last row g_m from Eq. (14) of the inverse matrix $\mathbf{G}^{-1}$ to the right part of the system of Eq. (A5) gives the first and last elements of the solution vector:

$$\begin{aligned}u_1^{(m)}&=\pm\frac{h}{2}v_m^{(m)}\langle\mathbf{y}^{*}|\tilde{\boldsymbol{\rho}}^{*}\rangle\mp\left(1+\frac{h}{2}u_1^{(m)}\right)\langle\mathbf{z}^{*}|\boldsymbol{\rho}\rangle,\\ v_m^{(m)}&=\pm\frac{h}{2}v_m^{(m)}\langle\tilde{\mathbf{z}}|\tilde{\boldsymbol{\rho}}^{*}\rangle-\left(1+\frac{h}{2}u_1^{(m)}\right)\langle\tilde{\mathbf{y}}|\boldsymbol{\rho}\rangle.\end{aligned} \tag{A7}$$

Here, angle brackets denote the convolution $\langle\mathbf{x}|\mathbf{y}\rangle=\mathbf{x}^{T}\cdot\mathbf{y}$. Note that $\langle\mathbf{y}^{*}|\tilde{\boldsymbol{\rho}}^{*}\rangle=\langle\tilde{\mathbf{y}}|\boldsymbol{\rho}\rangle^{*}$ and $\langle\tilde{\mathbf{z}}|\tilde{\boldsymbol{\rho}}^{*}\rangle=\langle\mathbf{z}^{*}|\boldsymbol{\rho}\rangle^{*}$, and the parameters are defined as

$$\alpha_m=h\langle\mathbf{z}^{*}|\rho\rangle,\qquad \beta_m=h\langle\tilde{\mathbf{y}}|\boldsymbol{\rho}\rangle. \tag{A8}$$

Solving Eq. (A7) for $u_1^{(m)}$ and $v_m^{(m)}$ we obtain

$$v_m^{(m)}=\frac{-\beta_m/h}{1\pm\operatorname{Im}\alpha_m-\frac{1}{4}(|\alpha_m|^2\mp|\beta_m|^2)}. \tag{A9}$$

Within the required order of accuracy $\alpha_m=-u(x_m,0)h+O(h^2)$. As follows from [37] (and an earlier paper [13]), function $u(x,0)=A_1(x,x)=\pm\int_{-\infty}^{x}|q(s)|^2\mathrm{d}s$ is real. Thus, $q_m=2v_m^{(m)}=-2\beta_m/h+O(h^2)$.

ACKNOWLEDGMENTS

This work was supported by Grant of Ministry of Education and Science of the Russian Federation (agreement no. 14.B25.31.0003), the Government program of the leading research schools NSh-4373.2014.2, and by the Russian Academy of Sciences through program # 24 of its Presidium and grants from its Division of Physical Sciences and Siberian Branch.

REFERENCES AND NOTES

1. G. P. Agrawal, *Nonlinear Fiber Optics* (Elsevier, 2007).
2. T. Taha, "Numerical simulation of the nonlinear Schrödinger equation," Math. Comput. Simul. **32**, 309–312 (1990).
3. E. Ding and J. N. Kutz, "Operating regimes, split-step modeling, and the Haus master mode-locking model," J. Opt. Soc. Am. B **26**, 2290–2300 (2009).
4. P. M. Lushnikov, "Fully parallel algorithm for simulating dispersion-managed wavelength-division-multiplexed optical fiber systems," Opt. Lett. **27**, 939–941 (2002).
5. A. O. Korotkevich and P. M. Lushnikov, "Proof-of-concept implementation of the massively parallel algorithm for simulation of dispersion-managed WDM optical fiber systems," Opt. Lett. **36**, 1851–1853 (2011).
6. E. G. Turitsyna and S. K. Turitsyn, "Digital signal processing based on inverse scattering transform," Opt. Lett. **38**, 4186–4188 (2013).
7. J. E. Prilepsky, S. A. Derevyanko, K. J. Blow, I. Gabitov, and S. K. Turitsyn, "Nonlinear inverse synthesis and eigenvalue division multiplexing in optical fiber channels," Phys. Rev. Lett. **113**, 013901 (2014).
8. M. Yousefi and F. Kschischang, "Information transmission using the nonlinear Fourier transform, part II: Numerical methods," IEEE Trans. Inf. Theory **60**, 4329–4345 (2014).
9. R. Feced, M. N. Zervas, and M. A. Muriel, "An efficient inverse scattering algorithm for the design of nonuniform Bragg gratings," IEEE J. Quantum Electron. **35**, 1105–1115 (1999).
10. L. Poladian, "Iterative and noniterative design algorithms for Bragg gratings," Opt. Fiber Technol. **5**, 215–222 (1999).
11. J. Skaar, L. Wang, and T. Erdogan, "On the synthesis of fiber Bragg gratings by layer peeling," IEEE J. Quantum Electron. **37**, 165–173 (2001).
12. A. Rosenthal and M. Horowitz, "Inverse scattering algorithm for reconstructing strongly reflecting fiber Bragg gratings," IEEE J. Quantum Electron. **39**, 1018–1026 (2003).
13. G. H. Song and S. Y. Shin, "Design of corrugated waveguide filters by the Gel'fand–Levitan–Marchenko inverse scattering method," J. Opt. Soc. Am. A **2**, 1905–1915 (1985).
14. F. Ahmad and M. Razzagh, "A numerical solution to the Gel'fand–Levitan–Marchenko equation," Appl. Math. Comput. **89**, 31–39 (1998).
15. P. Frangos and D. Jaggard, "A numerical solution to the Zakharov–Shabat inverse scattering problem," IEEE Trans. Antennas Propag. **39**, 74–79 (1991).
16. G. B. Xiao and K. Yashiro, "An efficient algorithm for solving Zakharov–Shabat inverse scattering problem," IEEE Trans. Antennas Propag. **50**, 807–811 (2002).
17. C. Papachristos and P. Frangos, "Design of corrugated optical waveguide filters through a direct numerical solution of the coupled Gel'fand–Levitan–Marchenko integral equations," J. Opt. Soc. Am. A **19**, 1005–1012 (2002).
18. A. Buryak, J. Bland-Hawthorn, and V. Steblina, "Comparison of inverse scattering algorithms for designing ultrabroadband fibre Bragg gratings," Opt. Express **17**, 1995–2004 (2009).
19. O. V. Belai, L. L. Frumin, E. V. Podivilov, and D. A. Shapiro, "Efficient numerical method of the fiber Bragg grating synthesis," J. Opt. Soc. Am. B **24**, 1451–1457 (2007).
20. V. E. Zakharov and A. B. Shabat, "Exact theory of two-dimensional self-focusing and one-dimensional self-modulation of waves in nonlinear media," Zh. Eksp. Teor. Fiz. **61**, 118–134 (1971).
21. N. Levinson, "The Wiener RMS error criterion in filter design and prediction," J. Math. Phys. **25**, 261–278 (1947).
22. J. Durbin, "The fitting of time series models," Rev. Inst. Int. Stat. **28**, 233 (1960).
23. W. F. Trench, "An algorithm for the inversion of finite Toeplitz matrices," SIAM J. Appl. Math. **12**, 515–522 (1964).
24. V. V. Voevodin and E. E. Tyrtyshnikov, *Toeplitz Matrices and Their Applications* (North-Holland, 1984).
25. R. E. Blahut, *Fast Algorithms for Digital Signal Processing* (Addison-Wesley, 1985).
26. O. V. Belai, E. V. Podivilov, L. L. Frumin, and D. A. Shapiro, "Numerical reconstruction stability of fiber Bragg gratings," Opt. Spectrosc. **105**, 103–110 (2008).
27. S. T. Le, J. E. Prilepsky, and S. K. Turitsyn, "Nonlinear inverse synthesis for high spectral efficiency transmission in optical fibers," Opt. Express **22**, 26720–26741 (2014).
28. R. Kashyap, *Fiber Bragg Gratings* (Academic, 1999).
29. S. Burtsev, R. Camassa, and I. Timofeyev, "Numerical algorithms for the direct spectral transform with applications to nonlinear Schrödinger type systems," J. Comput. Phys. **147**, 166–186 (1998).
30. G. L. Lamb, Jr., *Elements of Soliton Theory* (Wiley, 1980).
31. G. Boffetta and A. Osborne, "Computation of the direct scattering transform for the nonlinear Schrödinger equation," J. Comput. Phys. **102**, 252–264 (1992).

32. O. V. Belai, L. L. Frumin, E. V. Podivilov, O. Y. Schwarz, and D. A. Shapiro, "Finite Bragg grating synthesis by numerical solution of Hermitian Gel'fand–Levitan–Marchenko equations," J. Opt. Soc. Am. B **23**, 2040–2045 (2006).
33. A matrix with noncommuting blocks generally has different left and right inverse matrices.
34. E. V. Podivilov, D. A. Shapiro, and D. A. Trubitsyn, "Exactly solvable profiles of quasi-rectangular Bragg filter with dispersion compensation," J. Opt. A Pure Appl. Opt. **8**, 788–795 (2006).
35. F. W. J. Ovler, D. W. Lozier, R. F. Boisvert, and C. W. Clark, *NIST Handbook of Mathematical Functions* (Cambridge University, 2010).
36. S. Wahls and H. V. Poor, "Introducing the fast nonlinear Fourier transform," in *Proceedings of the IEEE International Conference on Acoustics, Speech, and Signal Processing (ICASSP)*, (IEEE, 2013), pp. 5780–5784.
37. A. Rosenthal and M. Horowitz, "Reconstruction of a fiber Bragg grating from noisy reflection data," J. Opt. Soc. Am. A **22**, 84–92 (2005).